Plant Soil
https://doi.org/10.1007/s11104-023-06201-5

METHODS PAPER

Laboratory μ-X-ray fluorescence elemental mapping of herbarium specimens for hyperaccumulator studies

Antony van der Ent · Lachlan W. Casey · Imam Purwadi · Peter D. Erskine

Received: 27 May 2023 / Accepted: 28 July 2023

Abstract

Background and aims An innovative approach "Herbarium Ionomics" used a handheld X-ray fluorescence (XRF) device to non-destructively extract quantitative elemental data (i.e., the metallome) from herbarium specimens. This has led to the discovery of numerous hyperaccumulator plants. Once a new hyperaccumulator is identified through XRF screening, the next step is to verify whether this is in fact 'real' as there are numerous causes for anomalous measurements caused by artefacts.

Methods Here we report on the use of a scanning μ-XRF for herbarium specimens to answer the question whether the abnormal concentrations of a particular element truly represent hyperaccumulation as well as reveal broad patterns of elemental distribution to provide the first hints at the ecophysiology of the hyperaccumulated element.

Results and conclusions The use of μ-XRF analysis of herbarium specimens can form the starting point for further studies using specimens properly prepared for micro-analytical investigations.

Keywords Elementome · Ionome · Metallome · XRF

Responsible Editor: Hans Lambers.

A. van der Ent (✉)
Laboratory of Genetics, Wageningen University and Research, Wageningen, The Netherlands
e-mail: antony.vanderent@wur.nl

A. van der Ent
Laboratoire Sols et Environnement, INRAE, Université de Lorraine, Nancy, France

A. van der Ent · I. Purwadi · P. D. Erskine
Centre for Mined Land Rehabilitation, Sustainable Minerals Institute, The University of Queensland, Brisbane, Queensland, Australia

L. W. Casey
Centre for Microscopy and Microanalysis, The University of Queensland, Brisbane, Australia

Introduction

Herbarium XRF Ionomics is a recently developed approach to obtain elemental data herbarium specimens to aid in the discovery of trace element hyperaccumulator plants (van der Ent et al. 2019a).

Since its inception, this approach has led to a doubling of the number of hyperaccumulator plants (Baker and Brooks 1989; van der Ent et al. 2013) known globally through scanning campaigns in New Caledonia, Malaysia, and Central America (McCartha et al. 2019; van der Ent et al. 2019b; Do et al. 2020; Gei et al. 2020). Once abnormal concentrations of a particular element are identified in specimen, the next step is to verify whether this is observation in fact 'real'. There are numerous causes for anomalous measurements caused by artefacts. Principal among the reasons why apparent extremely high

Published online: 23 August 2023

values may be obtained is dust contamination that adheres to the outside of the leaves. Even stringent washing of leaves (not typically done for herbarium specimens) cannot fully remove all dust, particularly if the dust is embedded in the waxy cuticle or between trichomes (Reeves and Kruckeberg 2018; Paul et al. 2019). Bulk analysis of such 'suspect' specimens will invariably reveal high concomitant chromium (Cr), iron (Fe), and titanium (Ti) concentrations, which are typical for most soils (Cary & Kubota, 1990). When viewed using a light microscope these particulates are often visible, or when analysed by micro-X-ray fluorescence (μ-XRF) this contamination reveals itself as high concentration hotspots dominated by the aforementioned soil abundant elements. Other soil common elements, such as Al and Si, are also potentially good indicators for soil contamination, but these very light elements are difficult to detect with XRF due to air-path absorption, unless vacuum or helium atmosphere is used (this is technically possible, but difficult and expensive in the case of helium).

Highly anomalous results can also arise from specimens that are not visibly dirty, for example, sub-milligram quantities of pure Cu minerals as dust incorporated with the analysis of plant material is sufficient to make the plant appear as a Cu 'hyperaccumulator' (Reeves and Baker 2000). At a high-level of magnification, scanning electron microscopy with energy dispersive spectroscopy (SEM-EDS) can be used to determine whether surficial contamination is the cause for abnormal elemental concentrations in the plant material (van der Ent et al. 2018). For instance, this has unequivocally shown that *Haumaniastrum robertii* and *Aeolanthus biformifolius* are genuine hyperaccumulators, with exceptionally high concentrations of Cu and Co within cells inside tissues (van der Ent et al. 2019b).

Older herbarium specimens have often been treated with mercury chloride ($HgCl_2$) for long-term insect protection, which results in extremely high apparent Hg concentrations in these specimens (i.e., >500 μg g^{-1}). In addition, some herbariums have used arsenic (As) compounds as a pesticide on specimens, similarly leading to very high As values. We have also encountered zinc (Zn)-rich glue being used to adhere specimens to cardboard which confounded the handheld XRF results for this element in herbarium specimens measured (van der Ent et al. 2019c). In many tropical countries in particular, herbarium specimens may be temporarily stored in methylated spirit during and immediately after collection to prevent decomposition. Typically, specimens are packed between old newspaper which is then soaked in methylated spirit and the package encapsuled within a large ZIP-lock bag. On arrival at the herbarium, specimens are removed from the bag, the methylated spirit is allowed to evaporate and the specimens are then oven dried. It is not known to what degree elements (and which elements) are potentially leached out from this process. Specimens treated in this way are normally readily identifiable because of the characteristic yellow discolouration (due to degradation of chlorophyll).

The method of specimen preparation (dehydration using an oven) is evidentially not congruent for observation of elemental distribution patterns at the scale of cells (e.g., 10s-micron scale), as structures and elemental redistribution occurred in the specimen. This has been forcefully shown in an example in van der Ent et al. (2018) in which tissue cross-sections were prepared by either air-drying or low-temperature freeze-drying (lyophilization). It shows the drastic differences with major shrinkage and redistribution of elements. Problematically, the elemental distribution in such specimens appear deceptively plausible, even though it is entirely artefactual. Although there is a distinct lack of this type of methodological studies, it seems highly unlikely that ions (even those that are highly mobile, such as K) will migrate more than a few cells spatially in distance. Elements that are present in the form of insoluble deposits, for example, as calcium-oxalate crystals, will likely not migrate at all.

Laboratory μ-XRF analysis can be used to determine elemental concentrations quantitatively and non-destructively. The method relies on illuminating a sample with a microbeam of X-rays, which excite electrons producing characteristic XRF of elements from the sample that can be analysed for understanding the composition of the sample/specimen. As such, μ-XRF analysis of herbarium specimens can be used to answer the question whether the abnormal concentrations of a particular element (from either bulk analysis or handheld XRF scanning) truly represent hyperaccumulation, or whether it is the result of artefacts. It can reveal broad patterns of elemental distribution, such as localization of the elemental distribution and provide the first hints at

the ecophysiology of the hyperaccumulated element. In this article we show three examples of laboratory μ-XRF analysis applied to herbarium specimens to highlight the usefulness of this method and encourage other scientists to explore this approach in their research.

Materials and methods

The UQ μ-XRF facility is a custom-built system manufactured by IXRF which consists of two 50 kV–1000 μA sources fitted with polycapillary focusing optics including a microfocus Mo-target tube producing 17.4 keV X-rays (flux of 2.2×10^8 ph s^{-1}) focusing to 25 μm which was used here. The system is fitted with two silicon drift detectors (SDD) of 150 mm^2 coupled to a XIA Mercury X4 signal processing unit. The fast motion stage can address areas up to 300×300 mm. Per pixel dwell times are typically 50–100 ms and each elemental map took 24–30 hrs to acquire.

Herbarium specimens (*Coelospermum decipiens*, *Crotalaria novo-hollandiae, Denhamia cunninghamii*) were on loan from the Queensland Herbarium (BRI). The herbarium specimens were not removed from the herbarium sheet and mounted by gently adhering them to the Perspex sample holder frame with double-sided sticky tape The cardboard was also scanned with the specimen, but this is of no consequence in this case, as it contains very low concentrations of transition elements (such as Mn, Zn) and heavy elements (such As, Cd) that could hyperaccumulated. However, the cardboard does contain appreciable K and Ca, but the fluorescent X-rays of these elements have a very low energy and normally do not penetrate through the herbarium specimen to the detector and are hence invisible in the elemental map of the specimen. In addition, leaves of *Macadamia integrifolia* (from a tree growing at St Lucia, Brisbane) were scanned in fresh hydrated state and following on immersed in methylated spirit (95% ethanol) for 24 hrs and then scanned again. The XRF spectra on the UQ microXRF facility (Fig. 1) were acquired in mapping mode using the instrument control package, Iridium (IXRF systems), and then imported into the GeoPIXE software package version 7.5 s (beta). The XRF spectra were subsequently fitted using the Dynamic Analysis method (Reeves and Baker 2000; Ryan and Jamieson 1993; Ryan et al. 1990, 2005). This method generates elemental images in with the Mo-tube Bremsstrahlung background has been subtracted.

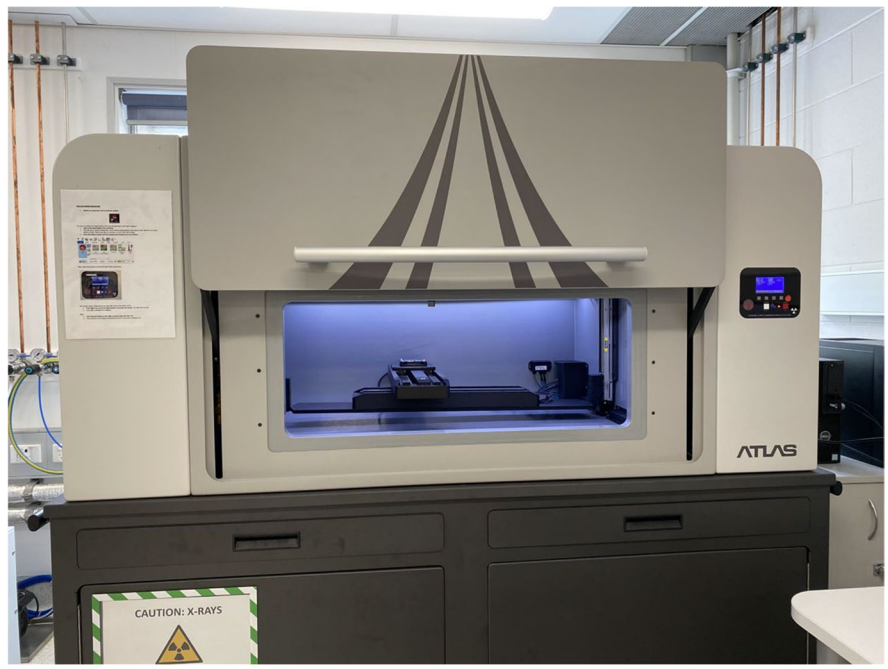

Fig. 1 The laboratory μ-X-ray fluorescence instrumentation used in this study showing the large sample chamber with the motion stage onto which samples are mounted for the analysis

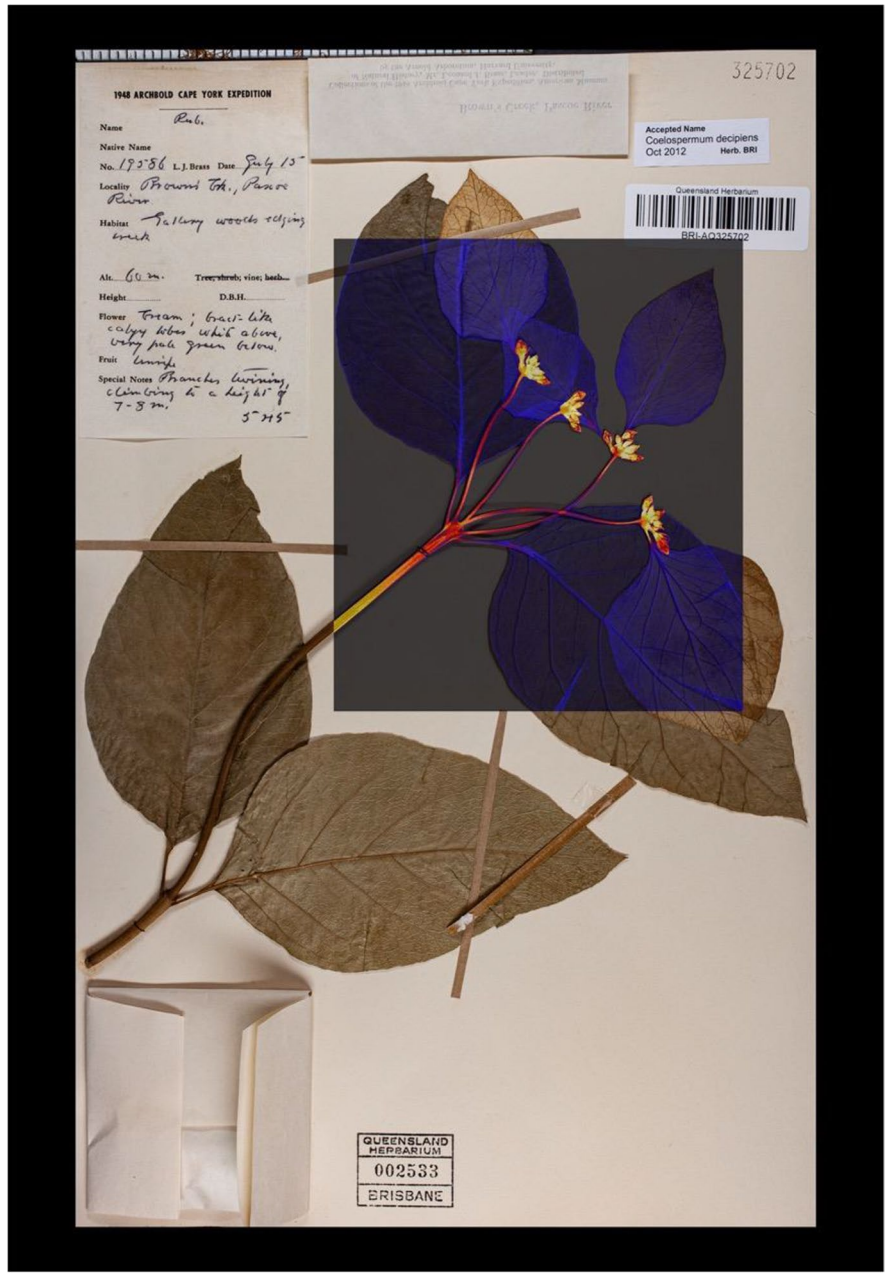

Fig. 2 Laboratory μ-X-ray fluorescence elemental map (1300 × 1129 pixels) overlaid over a photograph of an herbarium specimen (*Coelospermum decipiens*) that was found to hyperaccumulate Se. The brighter shades in the elemental map denote higher Se concentrations

Results

Three examples are shown and discussed here that have been analysed using the μ-XRF facility. In the first case, specimens of the genus *Coelospermum* (Rubiaceae) were XRF scanned at the Queensland Herbarium to determine selenium (Se) accumulation (Fig. 2), as one taxon (*C. decipiens)* in this genus is known to hyperaccumulate Se (Knott and McCray 1959; Peterson and Butler 1971). The elemental map derived from the μ-XRF analysis clearly shows that Se is most strongly enriched in the inflorescences, as well as in the stem, but is low in the leaves and in the floral bracts. The extremely high enrichment of Se in the flowers is characteristic for many Se hyperaccumulators and is, for example also seen in *Astragalus bisulcatus* (Valdez Barillas et al. 2012), but was not known previously from *C. decipiens*.

Fig. 3 Laboratory μ-X-ray fluorescence elemental map (1900 × 983 pixels) overlaid over a photograph of an herbarium specimen (*Crotalaria novo-hollandiae*) that was found to hyperaccumulate Zn. The brighter shades in the elemental map denote higher Se concentrations

The second example pertains to the facultative Zn hyperaccumulator *Crotalaria novo-hollandiae* (Fabaceae), shown in Fig. 3. Hyperaccumulation of Zn in this taxon is restricted to a few occurrences on Zn-Pb gossans that are naturally enriched in Zn where it can attain up to 16,200 μg g^{-1} Zn in its leaves (Tang et al. 2022). This herbarium specimen was originally collected in 1976 from the Dugald River Zn-Pb mineralized outcrop near Cloncurry in central Queensland, Australia. The μ-XRF element map shows that Zn is concentrated in the vascular bundles and Zn concentrations are highest in older leaves, and distinctly low in the floral spikes and very low in the inflorescences. The last example (Fig. 4) shows the distribution of Mn in *Denhamia cunninghamii* (Celastraceae), a species that can accumulate up to 32,000 μg g^{-1} Mn in its leaves (Abubakari et al. 2021). The μ-XRF elemental map illustrates

Fig. 4 Laboratory μ-X-ray fluorescence elemental map (2200 × 1660 pixels) overlaid over a photograph of an herbarium specimen (*Denhamia cunninghamii*) that was found to hyperaccumulate Mn. The brighter shades in the Mn elemental map denote higher concentrations

that Mn is highest towards the apex of each leaf, with a clear concentration gradient towards the base of the leaf. This is very similar to results of μ-XRF analysis of fresh hydrated material of *D. cunninghamii* (Abubakari et al. 2021). In the image it can be seen that blobs of glue used to adhere the specimen to then cardboard absorbed emitted Mn fluorescence signal from the underlying leaf, resulting in apparent circular Mn 'depletion' artefacts. Each of these three cases concerns hyperaccumulators in which shoot metal(loid) concentrations are much higher than soil concentration, thus excluding the possibility of any important contribution from soil particle contamination. Moreover, in all of the specimens none had visible Fe or Cr dust contamination (data not shown).

It is common for herbarium specimens to be preserved in methylated spirit after field collection to prevent decomposition. The specimens are

then pressed and dried. It is highly probable that this results in major elemental, re-distribution, especially of 'mobile' (soluble) elements. Therefore, we tested this by μ-XRF analysis of fresh/hydrated leaves of *Macadamia integrifolia* followed by immersion in ethanol for 24 hrs and then μ-XRF analysis again. We did not dry the leaves prior to the first scan so as to best emulate what happens with actual herbarium specimens (which are also immersed in ethanol when in hydrated state and then dried). We show the distributions of a highly mobile element (K), a non-mobile element (Ca)

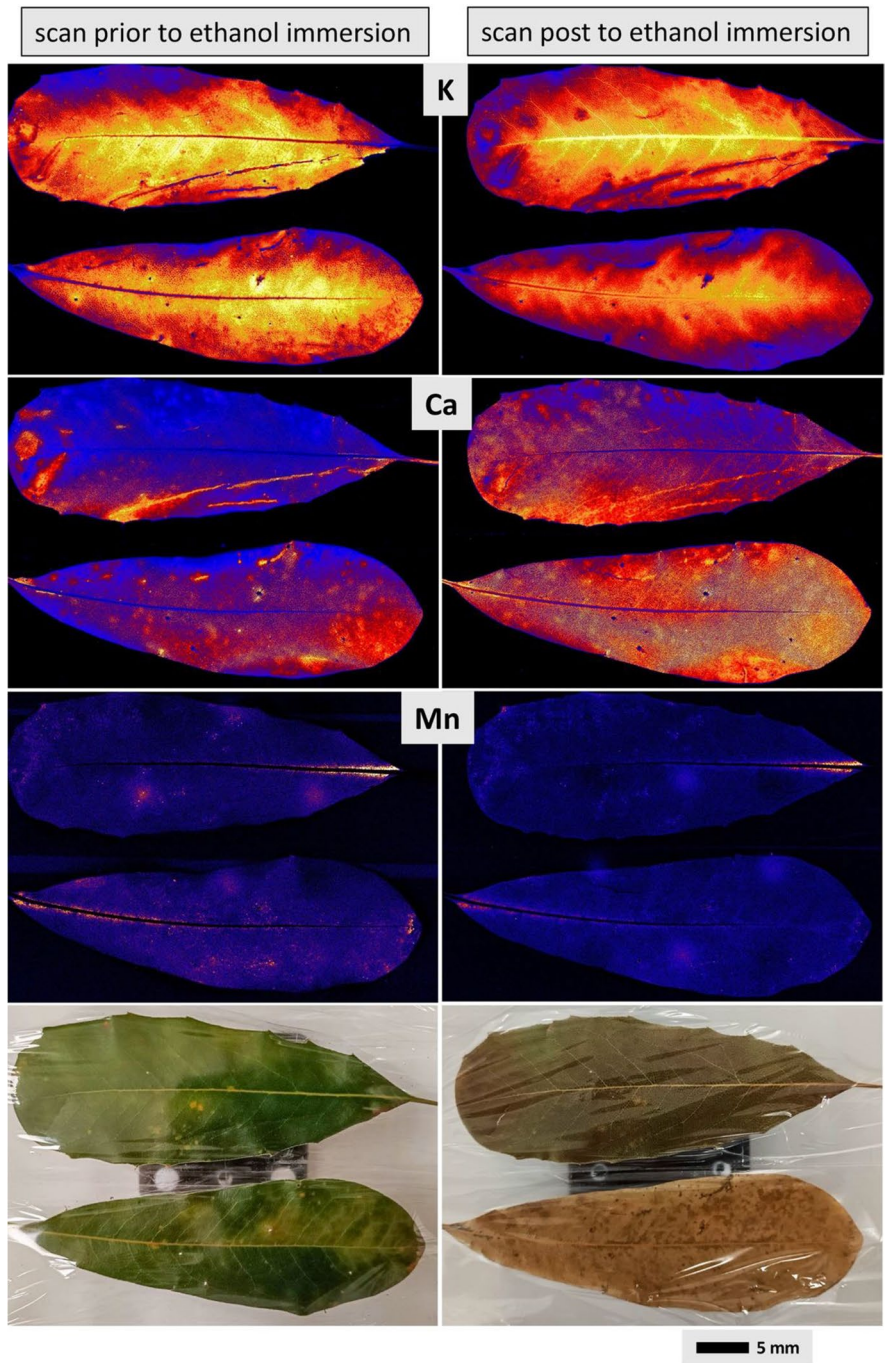

Fig. 5 Laboratory μ-X-ray fluorescence elemental maps of K, Ca, and Mn of leaves of *Macadamia integrifolia* before after and immersion in methylated spirit (95% ethanol). Images of the leaves are also shown. The brighter shades in the elemental map denote higher concentrations

and a trace element (Mn) with unknown mobility in Fig. 5. It is apparent that for both K and Ca the drying of the leaves resulted in lower absorption of the low-energy fluorescence X-rays and scattering due to water. This results in better 'definition' in fine scale patterns of the distribution of these elements. This is especially visible in the Ca maps where Ca-crystalline deposits lining the fine vasculature of the leaves are more visible in the dried ethanol immersed leaf. It is also clear that some K is depleted in areas where there is damage in the leaves, likely due to 'leaking out'. The maps of Mn look very similar. The changes induced by ethanol immersion are less pronounced than we expected and *grosso modo* overall patterns of elemental distribution are very similar before and after ethanol immersion. That means that even herbarium specimens treated with methylated spirit could be examined, but caution still applies when interpreting the results.

Discussion

The use of laboratory µ-XRF analysis of herbarium specimens can form the starting point for further studies using specimens properly prepared for micro-analytical investigations. The examples illustrated here provide a case in point on how this approach may assist in investigating abnormal metal accumulation in plants and rule out extraneous contamination. Of course, the use of this method relies on the (local) availability of this instrumentation. However, costs are comparable to that of routinely used analytical infrastructure, such as ICP-MS, it is non-destructive and it is significantly cheaper than SEM-EDS, and likely to become widely accessible in the near future.

Acknowledgements We acknowledge the support and instrumentation provided by Microscopy Australia at the Center for Microscopy and Microanalysis at the University of Queensland. We thank the Director of the Queensland Herbarium, Department of Environment and Sciences, Queensland Government, for loan of the specimens for µXRF analysis.

Author contributions AVDE and LWC designed and conducted the experiment. AVDE, IP and PDE wrote the manuscript.

Funding Imam Purwadi was the recipient of an Australian Government Research Training Program Scholarship and Graduate School Scholarships at The University of Queensland, Australia. This work was supported by the French National Research Agency through the national program "Investissements d'avenir" (ANR-10-LABX-21 - RESSOURCES21). A. van der Ent acknowledges The Australian Academy of Science for the 2021 Thomas Davies Research Grant for Marine, Soil and Plant Biology which funded part of this project.

Declarations

Conflict of interest The authors declare no conflicts of interest relevant to the content of this manuscript.

References

Abubakari F, Nkrumah PN, Erskine PD, Brown GK, Fernando DR, Echevarria G, van der Ent A (2021) Manganese (hyper)accumulation within Australian *Denhamia* (Celastraceae): an assessment of the trait and manganese accumulation under controlled conditions. Plant Soil 463(1):205–223. https://doi.org/10.1007/s11104-021-04833-z

Baker AJM, Brooks RR (1989) Terrestrial higher plants which hyperaccumulate metallic elements – a review of their distribution, ecology, and phytochemistry. Biorecovery 1:81–126

Cary EE, Kubota J (1990) Chromium concentration plants: effects of soil chromium concentration and tissue contamination by soil. J Agric Food Chem 38(1):108–114. https://doi.org/10.1021/jf00091a022

Do C, Abubakari F, Remigio AC, Brown GK, Casey LW, Burtet-Sarramegna V, Gei V, Erskine PD, van der Ent A (2020) A preliminary survey of nickel, manganese and zinc (hyper)accumulation in the flora of Papua New Guinea from herbarium X-ray fluorescence scanning. Chemoecology 30:1–13. https://doi.org/10.1007/s00049-019-00293-1

Gei V, Isnard S, Erskine PD, Echevarria G, Fogliani B, Jaffré T, van der Ent A (2020) A systematic assessment of the occurrence of trace element hyperaccumulation in the flora of New Caledonia. Bot J Linn Soc 194:1–22. https://doi.org/10.1093/botlinnean/boaa029

Knott S, McCray C (1959) Two naturally occurring outbreaks of selenosis in Queensland. Aust Vet J 35:161–165

McCartha GL, Taylor CM, van der Ent A, Echevarria G, Navarrete Gutiérrez DM, Pollard AJ (2019) Phylogenetic and geographic distribution of nickel hyperaccumulation in neotropical *Psychotria*. Am J Bot 106:1377–1385

Paul ADL, van der Ent A, Erskine PD (2019) Scandium biogeochemistry at the Lucknow laterite plateau, Queensland, Australia. J Geochem Explor 204:74–82. https://doi.org/10.1016/j.gexplo.2019.05.005

Peterson PJ, Butler GW (1971) The occurrence of selenocystathionine in *Morinda reticulata* benth., a toxic seleniferous plant. Aust J Biol Sci 24:175–177

Reeves RD, Baker AJM (2000) Metal-accumulating plants. In: Raskin I, Ensley BD (eds) Phytoremediation of toxic metals: using plants to clean up the environment. Wiley, New York, pp 193–229

Reeves RD, Kruckeberg AR (2018) Re-examination of the elemental composition of some Caryophyllaceae on north American ultramafic soils. Ecol Res 33:715–722. https://doi.org/10.1007/s11284-017-1556-y

Ryan CG (2000) Quantitative trace element imaging using PIXE and the nuclear microprobe. Int J Imaging Syst Technol 11:219-230. https://hdl.handle.net/102.100.100/209480

Ryan CG, Jamieson DN (1993) Dynamic analysis: on-line quantitative PIXE microanalysis and its use in overlap-resolved elemental mapping. Nucl Instrum Methods Phys Res B 77(1–4):203–214. https://doi.org/10.1016/0168-583X(93)95545-G

Ryan CG, Cousens DR, Sie SH, Griffin WL (1990) Quantitative analysis of PIXE spectra in geoscience applications. Nucl Instrum Methods Phys Res B 49(1–4):271–276. https://doi.org/10.1016/0168-583X(90)90259-W

Ryan CG, Etschmann BE, Vogt S, Maser J, Harland CL, Van Achterbergh E, Legnini D (2005) Nuclear microprobe—synchrotron synergy: towards integrated quantitative real-time elemental imaging using PIXE and SXRF. Nucl Instrum Methods Phys Res B 231(1–4):183–188. https://doi.org/10.1016/j.nimb.2005.01.054

Tang RH, Erskine PD, Nkrumah PN, Echevarria G (2022) Van der Ent a (2022) soil-plant relationships of metallophytes of the zinc-lead-copper Dugald River gossan, Queensland. Australia Plant Soil 471:227–245. https://doi.org/10.1007/s11104-021-05209-z

Valdez Barillas JR, Quinn CF, Freeman JL, Lindblom SD, Fakra SC, Marcus MA, Gilligan TM, Alford ER, Wangeline AL, Pilon-Smits EAH (2012) Selenium distribution and speciation in the Hyperaccumulator *Astragalus bisulcatus* and associated ecological partners. Plant Physiol 159(4):1834–1844. https://doi.org/10.1104/pp.112.199307

van der Ent A, Reeves RD, Baker AJM, Pollard J, Schat H (2013) Hyperaccumulators of metal and metalloid trace elements: facts and fiction. Plant Soil 362(1–2):319–334. https://doi.org/10.1007/s11104-012-1287-3

van der Ent A, Przybyłowicz WJ, de Jonge MD, Harris HH, Ryan CG, Tylko G, Paterson DJ, Barnabas AD, Kopittke, PM Mesjasz-Przybyłowicz J (2018) X-ray elemental mapping techniques for elucidating the ecophysiology of hyperaccumulator plants. New Phytol 218:432–452. https://doi.org/10.1111/nph.14810

van der Ent A, Echevarria G, Pollard AJ, Erskine PD (2019a) X-ray fluorescence Ionomics of herbarium collections. Sci Rep 9:4746. https://doi.org/10.1038/s41598-019-40050-6

van der Ent A, Erskine PD, Malaisse F, Mesjasz-Przybylowicz J, Przybylowicz WJ, Barnabas AD, Sosnicka M, Harris HH (2019b) Abnormal concentrations of cu-co in *Haumaniastrum katangense*, *Haumaniastrum robertii* and *Aeolanthus biformifolius*: contamination or hyperaccumulation? Metallomics 11:586–596. https://doi.org/10.1039/c8mt00300a

van der Ent A, Ocenar A, Tisserand R, Sugau JB, Erskine PD, Echevarria G (2019c) Herbarium X-ray fluorescence screening for nickel, cobalt and manganese hyperaccumulation in the flora of Sabah (Malaysia, Borneo Island). J Geochem Explor 202:49–58. https://doi.org/10.1016/j.gexplo.2019.03.013